

# Rate Determination in Phosphorylation of Shark Rectal Na,K-ATPase by ATP: Temperature Sensitivity and Effects of ADP

Flemming Cornelius

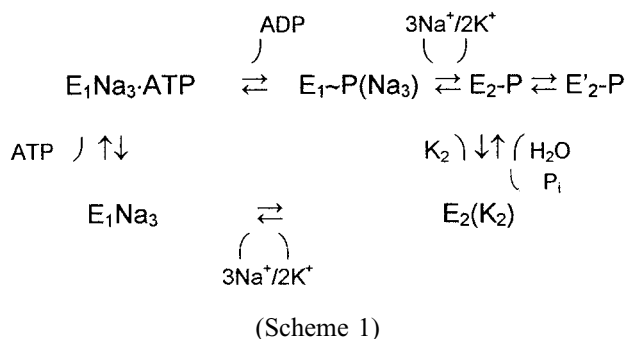
Department of Biophysics, University of Aarhus, DK-8000 Aarhus C, Denmark

**ABSTRACT** Phosphorylation of shark rectal Na,K-ATPase by ATP in the presence of  $\text{Na}^+$  was characterized by chemical quench experiments and by stopped-flow RH421 fluorescence. The appearance of acid-stable phosphoenzyme was faster than the rate of fluorescence increase, suggesting that of the two acid-stable phosphoenzymes formed, RH421 exclusively detects formation of  $\text{E}_2\text{-P}$ , which follows formation of  $\text{E}_1\text{-P}$ . The stopped-flow RH421 fluorescence response to ATP phosphorylation was biphasic, with a major fast phase with  $k_{\text{obs}} \sim 90 \text{ s}^{-1}$  and a minor slow phase with a  $k_{\text{obs}}$  of  $\sim 9 \text{ s}^{-1}$  (20°C, pH 7.4). The observed rate constants for both the slow and the fast phase could be fitted with identical second-degree functions of the ATP concentration with apparent binding constants of  $\sim 3.1 \times 10^7 \text{ M}^{-1}$  and  $1.8 \times 10^5 \text{ M}^{-1}$ , respectively. Increasing [ADP] decreased  $k_{\text{obs}}$  for the rate of the RH421 fluorescence response to ATP phosphorylation. This could be accounted for by the reaction of ADP with the initially formed  $\text{E}_1\text{-P}$  followed by a conformational change to  $\text{E}_2\text{-P}$ . The biphasic stopped-flow RH421 responses to ATP phosphorylation could be simulated, assuming that in the absence of  $\text{K}^+$  the highly fluorescent  $\text{E}_2\text{-P}$  is slowly transformed into the “ $\text{K}^+$ -insensitive”  $\text{E}'_2\text{-P}$  subconformation forming a side branch of the main cycle.

## INTRODUCTION

The  $\text{Na}^+, \text{K}^+$ -ATPase is the membrane bound protein found in all higher animal cells that maintains the ion gradients for  $\text{Na}^+$  and  $\text{K}^+$  across the cell membrane at the expenditure of energy derived from the splitting of ATP (Skou, 1992; Cornelius, 1996). It belongs to the P-type ATPases characterized by a phosphoryl transfer reaction in which the  $\gamma$ -phosphate from ATP is reacting with a  $\beta$ -carboxyl group of an aspartyl residue (Asp-369) at a high-affinity ATP substrate site on the protein (Albers, 1967; Post et al., 1969). The phosphoenzyme initially produced contains a covalent “high-energy” acyl-phosphate bond and is denoted  $\text{E}_1\text{-P}$  (or just  $\text{E}_1\text{P}$ ) and can donate its phosphate group in a reversible reaction to ADP. This phosphoform is spontaneously transformed into the “low-energy”  $\text{E}_2\text{-P}$  phosphoenzyme that can only donate its phosphate to water in a dephosphorylation reaction strongly activated by  $\text{K}^+$ . The phosphorylation/dephosphorylation reactions of the  $\text{Na}^+, \text{K}^+$ -ATPase are obligatorily coupled to vectorial transports of 3  $\text{Na}^+$  out of the cell and 2  $\text{K}^+$  into the cell (Jencks, 1983) as depicted in

Scheme 1:



In the absence of  $\text{K}^+$  the dephosphorylation of  $\text{E}_2\text{P}$  is slow,  $\sim 1.1 \text{ s}^{-1}$  (Cornelius et al., 1998) and as a side reaction of the main cycle a transition to the  $\text{K}^+$ -insensitive phosphoenzyme,  $\text{E}'_2\text{P}$  could become significant (Cornelius et al., 1998; Post et al., 1975; Fedosova et al., 1998). This  $\text{E}'_2\text{P}$  subconformation is the main phosphoenzyme formed when the enzyme is phosphorylated from  $\text{P}_i$ .

In the present paper the styryl dye RH421 that partitions into the lipid membrane and exhibits a high fluorescence when associated with  $\text{Na}^+, \text{K}^+$ -ATPase phosphoforms in either  $\text{E}_2\text{P}$  or  $\text{E}'_2\text{P}$  conformations (Forbush and Klodos, 1991; Stürmer et al., 1991; Fedosova et al., 1995; Kane et al., 1997; Clarke et al., 1998) is used to monitor the kinetics of the phosphorylation reaction of  $\text{Na}^+, \text{K}^+$ -ATPase by ATP in the presence of  $\text{Na}^+$ .

The detailed kinetics of  $\text{Na}^+, \text{K}^+$ -ATPase phosphorylation by ATP are still discussed in the literature. One point of controversy concerns which step in the phosphorylation reaction is rate-limiting. On the basis of comparisons between stopped-flow RH421 fluorescence measurements and quenched-flow measurements, Kane et al. (1997, 1998) suggested that for pig kidney  $\text{Na}^+, \text{K}^+$ -ATPase at pH 7.4 and 24°C the phosphorylation reaction is rate-limiting at

Received for publication 22 February 1999 and in final form 10 May 1999.

Address reprint requests to Dr. Flemming Cornelius, Department of Biophysics, University of Aarhus, Ole Worms Allé 185, DK-8000 Aarhus C, Denmark. Tel.: +45 8942 2926; Fax: +45 8612 9599; E-mail: fc@biophys.au.dk.

**Abbreviations used:**  $\text{E}_1$ , Na,K-ATPase form with high affinity toward ATP and  $\text{Na}^+$ ;  $\text{E}_2$ , Na,K-ATPase form with high affinity toward  $\text{K}^+$  and low affinity to ATP; EP, phosphoenzyme;  $\text{E}_1\text{-P}$ , ADP-sensitive phosphoenzyme;  $\text{E}_2\text{-P}$ ,  $\text{K}^+$ -sensitive phosphoenzyme;  $\text{E}'_2\text{-P}$ ,  $\text{K}^+$ -insensitive phosphoenzyme.

© 1999 by the Biophysical Society

0006-3495/99/08/934/09 \$2.00

saturating ATP, and  $\text{Na}^+$  followed by a rapid conformational change:  $\text{E}_1\text{Na}_3 + \text{ATP} \rightarrow \text{E}_1\text{P}(\text{Na}_3) \rightarrow \text{E}_2\text{P}(\text{Na}_3)$ . More specifically, Keillor and Jencks (1996) presented evidence from ADP effects on transient measurements of acid-stable phosphoenzyme production in the phosphorylation reaction, which indicated that the phosphoryl transfer is unlikely to be the rate-limiting step in the phosphorylation reaction. They suggested that the rate-limiting step for phosphorylation is a conformational transition between the initially formed  $\text{E}_1 \cdot \text{ATP}$  and a new enzyme species,  $\text{E}^* \cdot \text{ATP}$ , in the Albers-Post scheme (Albers, 1967; Post et al., 1969), which catalyses phosphoryl transfer at a very fast rate (Keillor and Jencks, 1996). Another controversial point concerns the biphasic time course of the ATP phosphorylation reaction: is it an artefact arising from a dye-protein interaction (Heyse et al., 1994), or is it an intrinsic kinetic property of the protein-substrate interaction (Kane et al., 1997; Clarke et al., 1998)?

In the present investigation these questions concerning the phosphorylation reaction with ATP in the presence of  $\text{Na}^+$  were addressed using shark rectal gland  $\text{Na}^+, \text{K}^+$ -ATPase, which is five times more sensitive to phosphorylation measured by RH421 than pig kidney enzyme (Klodos et al., 1997). This enabled a direct comparison of rapid mixing stopped-flow RH421 fluorescence with chemical quenched-flow data, and unambiguously demonstrated that under certain temperature conditions the fast phosphoryl transfer reaction is followed by a slower rate-determining conformational change. Also, the apparent controversial findings in the literature can probably be explained by a difference in the temperature sensitivity of the two reactions. Furthermore, the effects of ADP could be adequately accounted for by its interaction with the  $\text{E}_1\text{-P}$  phosphoenzyme in the classical Albers-Post model (Albers, 1967; Post et al., 1969). Finally, the slow phase in the stopped-flow RH421 fluorescence responses after ATP phosphorylation was found to be an intrinsic kinetic property of the protein-substrate interaction and could be modeled by a slow formation of  $\text{E}_2\text{P}$  in the absence of  $\text{K}^+$ .

## EXPERIMENTAL PROCEDURES

### Enzyme preparation

Na,K-ATPase (EC 3.6.1.37) from shark rectal glands was purified as previously described (Skou and Esmann, 1988). The specific hydrolytic activity measured at 37°C and under standard conditions according to Ottolenghi (1975) was 30–33 U/mg protein. The protein content was determined according to Lowry et al. (1951), using bovine serum albumin as standard.

### Materials

ATP was purchased as the sodium salt from Boehringer Mannheim, Germany, and purified and converted to the Tris salt by chromatography on a Dowex 1 column (Sigma Chemical Co., St. Louis, MO).  $[\gamma\text{-}^{32}\text{P}]\text{ATP}$  was from Amersham, U.K. RH421 was purchased from Molecular Probes, Inc., Eugene, OR, and dissolved in dimethyl sulfoxide. HEPES, MES, and *N*-methyl-D-glucamine were purchased from Sigma. All other reagents

were reagent grade. Quenched-flow phosphorylation of Na,K-ATPase from  $[\gamma\text{-}^{32}\text{P}]\text{ATP}$  (25  $\mu\text{M}$ ) was performed as previously described by Cornelius (1995) in a medium containing 1 mM  $\text{MgCl}_2$ , 16 mM NaCl, and 30 mM imidazole, pH 7.4.

## Steady-state and transient fluorescence measurements

Steady-state levels of RH421 fluorescence after the addition of ATP were measured using 50 mg/ml Na,K-ATPase in the presence of 16 mM NaCl, 4 mM  $\text{MgCl}_2$  in 10 mM HEPES, 10 mM MES, or 30 mM imidazole, adjusted with *N*-methyl-D-glucamine acid to pH 7.5. The responses were measured on a SPEX Fluorolog fluorometer in a cuvette (1-cm lightpath) with continuous stirring. The RH421 concentration was 260 nM.

Initial measurements of the RH421 fluorescence responses were performed using an SX.17MV rapid mixing stopped-flow spectrofluorometer (Applied Photophysics, U.K.). The flow volume was 100–300  $\mu\text{l}$ . The excitation wavelength was 546 nm (using a combined xenon/mercury lamp) and fluorescence was measured at emissions  $\geq 630$  nm using a cutoff filter. The dead time for the stopped-flow apparatus was  $\sim 1.5$  ms.

## Data analysis

The kinetic data were fitted with either monoexponential or double-exponential functions and the goodness of the fits were quantified using an *F*-test and a 5% confidence level. Biphasic kinetics can result from several different models and neither the observed rate constants nor the magnitude of the fast and slow phases in such fits can be ascribed to any single rate constant or pool-size in a kinetic model.

The fits of rate constants in kinetic models to stopped-flow RH421 fluorescence data were performed using the program DYNAFIT (Kuzmic, 1996). Simulation of kinetic models was performed with the program Chemical Kinetics Simulator (IBM Corporation, Armonk, NY).

## RESULTS AND DISCUSSION

It has previously been demonstrated that shark rectal  $\text{Na}^+, \text{K}^+$ -ATPase responds to ATP phosphorylation with an RH421 fluorescence change ( $\Delta F/F_0$ ) which is  $\sim 5$  times larger than for pig renal enzyme (Klodos et al., 1997). Shark rectal enzyme was, therefore, used to study the ATP phosphorylation kinetics in further detail comparing transient stopped-flow fluorescence response of RH421 with transient quenched-flow techniques.

### RH421 fluorescence associated with ATP phosphorylation

In Fig. 1 rapid mixing stopped-flow responses at 20°C to the addition of a saturating ATP concentration (300  $\mu\text{M}$ ) and 4 mM  $\text{Mg}^{2+}$  in the presence of 16 or 130 mM  $\text{Na}^+$  are shown. The concentration of RH421 (260 nM) used in these experiments was below the value ( $\approx 1$   $\mu\text{M}$ ) where a dye inhibition of steady-state enzyme activity can be observed (Frank et al., 1996). The fluorescence responses were significantly better fitted with double-exponential time functions with a large fast phase followed by a smaller slow phase than with monoexponentials, as also previously noted (Kane, 1997; Clarke et al., 1998; Heyse et al., 1994). As indicated, the observed rate constants for the fluorescence increase at 130 mM  $\text{Na}^+$  slightly exceed those calculated at 16 mM  $\text{Na}^+$ ,

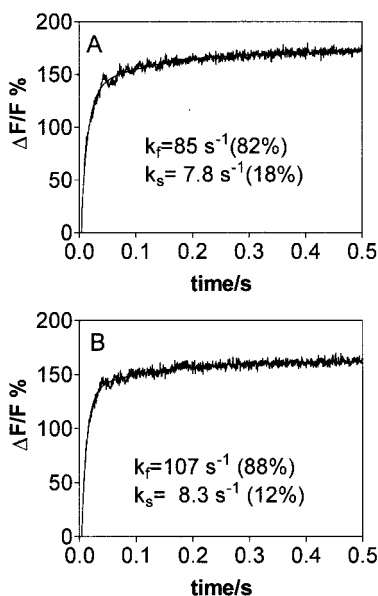


FIGURE 1 Rapid mixing stopped-flow RH421 fluorescence response of shark rectal gland  $\text{Na}^+, \text{K}^+$ -ATPase membrane fragments to ATP phosphorylation at 16 mM  $\text{Na}^+$  (A) or 130 mM  $\text{Na}^+$  (B). One syringe contained shark enzyme (0.067 mg/ml after mixing) in 16 mM or 130 mM NaCl, 4 mM  $\text{MgCl}_2$ , 10 mM HEPES/MES (pH 7.5), and 260 nM RH421. The other syringe contained the same solution plus 2 mM ATP (final concentration 1 mM).  $T = 20.2^\circ\text{C}$ . The traces show the increase in relative fluorescence compared to the initial fluorescence level and are the average of five stopped-flow experiments, each collecting 4000 data points. The RH421 fluorescence was measured using an excitation wavelength of 550 nm at emission wavelengths  $\geq 630$  nm. The curves represent double exponential fits to the data with observed rate constants ( $k_f$  and  $k_s$ ) and the fractions of slow and fast phases indicated.

indicating that 16 mM  $\text{Na}^+$  is subsaturating, as previously observed (Cornelius et al., 1998; Stürmer et al., 1991; Clarke et al., 1998) and as seen from Fig. 5 below. In nine experiments performed at 300  $\mu\text{M}$  ATP, 16 mM  $\text{Na}^+$ , 4 mM  $\text{Mg}^{2+}$ , 10 mM HEPES/MES, pH 7.5 the faster phase comprised a fraction of  $0.83 \pm 0.05$  with an observed rate constant of  $90.2 \pm 2.1 \text{ s}^{-1}$ , whereas the slower phase amounted to  $0.17 \pm 0.01$  with an observed rate constant of  $8.8 \pm 0.8 \text{ s}^{-1}$ . At identical conditions except for a higher  $\text{Na}^+$  concentration of 130 mM, the faster phase comprised a fraction of  $0.85 \pm 0.02$  with an observed rate constant of  $107 \pm 2 \text{ s}^{-1}$ , whereas the slower phase amounted to  $0.15 \pm 0.02$  with an observed rate constant of  $9.8 \pm 1.0 \text{ s}^{-1}$ . The measured rate constant for the major fast phase is comparable to previous values found using stopped-flow RH421 fluorescence measurements. Kane et al. (1997) found 160  $\text{s}^{-1}$  for pig kidney enzyme at  $24^\circ\text{C}$  and Clarke et al. (1998) found 200  $\text{s}^{-1}$  for rabbit enzyme, also at  $24^\circ\text{C}$ . Others, however, have found appreciably lower values of 18–30  $\text{s}^{-1}$  using photochemical release of caged ATP (Stürmer et al., 1991; Heyse et al., 1994; Bühler et al., 1991; Sokolov et al., 1998), which are apparently due to inhibition by unphosphorylated caged ATP (Clarke et al., 1998).

Clarke et al. (1998) attributed the faster phase of the biphasic response of stopped-flow RH421 fluorescence af-

ter ATP phosphorylation to the phosphorylation of the enzyme and the subsequent conformational change with release of 3  $\text{Na}^+$ :  $\text{E}_1\text{ATP}(\text{Na}_3) \rightarrow \text{E}_2\text{P}(\text{Na}_3) \rightarrow \text{E}_2\text{P}$ , whereas the slow phase was assigned to the relaxation of the dephosphorylation/rephosphorylation equilibrium:  $\text{E}_2\text{P} \rightarrow \text{E}_2 \rightarrow \text{E}_1 + 3 \text{Na}^+ \rightarrow \text{E}_1(\text{Na}_3) + \text{ATP} \rightarrow \text{E}_2\text{P}(\text{Na}_3) \rightarrow \text{E}_2\text{P} + 3 \text{Na}^+$ . The latter assumes that the fluorescence level of RH421 associated with  $\text{E}_2$  is as high as or higher than that of dye associated with  $\text{E}_2\text{P}$ . We have previously analyzed RH421 fluorescence results associated with phosphorylation from  $\text{P}_i$  and found that development of the fluorescent response corresponds to the formation of phosphoforms in  $\text{E}_2$  conformation (Cornelius et al., 1998; Fedosova et al., 1998). This is also in accord with experiments with chymotrypsin- or oligomycin-treated enzyme—both stabilizing  $\text{E}_1\text{-P}$ —that compared to control enzyme showed a decrease in the RH421 fluorescence level after the addition of ATP (Stürmer et al., 1991; Klodos, 1994; Pratap and Robinson, 1993).

### Quenched-flow experiments with ATP phosphorylation

In Fig. 2 quenched-flow experiments with ATP phosphorylation of shark  $\text{Na}^+, \text{K}^+$ -ATPase performed at 5, 10, and  $15^\circ\text{C}$  are shown and compared to stopped-flow RH421 fluorescence experiments performed under exactly identical conditions (25  $\mu\text{M}$  ATP, 16 mM  $\text{Na}^+$ , 1 mM  $\text{Mg}^{2+}$ , 30 mM imidazole, pH 7.4). At higher temperatures the quenched-flow responses were too fast to be accurately resolved. Although monoexponential time functions were adequate to fit the quenched-flow data, the observed rate constants should, therefore, only be regarded as lower limits. The observed rate constants adjusted to  $20^\circ\text{C}$  using an activation energy of 52 kJ/mol (see Fig. 3) give  $\sim 170 \text{ s}^{-1}$ , much the same as previously found by Kane et al. (1997). As clearly seen from Fig. 2, however, the initial rate of formation of acid-stable phosphoenzyme after ATP addition is much faster than the appearance of RH421 fluorescence measured by stopped-flow, as also previously found (Cornelius et al., 1998). It should be noted, also, that the difference in rates detected by RH421 fluorescence and quenched-flow measurement decreased progressively at increasing temperatures. Another feature noted from Fig. 2 is the presence of a clear lag phase in the RH421 fluorescence when phosphorylation is induced by a low ATP concentration, especially at low temperatures. These results indicate that the formation of the non- or low-fluorescent but acid-stable phosphoenzyme  $\text{E}_1\text{-P}$  is faster than formation of the high-fluorescent  $\text{E}_2\text{P}$ . The fact that both the time delay between formation of acid-stable phosphoenzyme and fluorescence and the lag-phase in RH421 fluorescence become more pronounced at lower temperatures indicate that the latter conformational change  $\text{E}_1\text{-P} \rightleftharpoons \text{E}_2\text{P}$  is more temperature-sensitive than the phosphoryl transfer reaction. Fig. 2 clearly demonstrates that phosphorylation is not the main

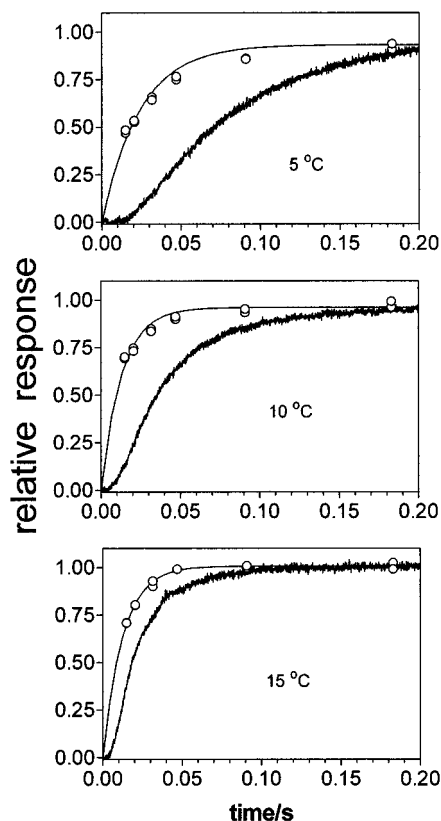


FIGURE 2 Comparison of ATP phosphorylation transients measured by either quenched-flow (○) or stopped-flow RH421 fluorescence at different temperatures (5, 10, and 15°C). The conditions were identical in the two experiments: 25  $\mu$ M ATP, 130 mM NaCl, 1 mM  $\text{MgCl}_2$ , 30 mM imidazole, pH 7.5. The responses were normalized. The curves are monoexponential fits to the quenched-flow data with observed rate constants: 5°C,  $41.8 \pm 2.1 \text{ s}^{-1}$ ; 10°C,  $77.4 \pm 3.4 \text{ s}^{-1}$ ; and 15°C,  $79.4 \pm 1.7 \text{ s}^{-1}$ . For quenched-flow, duplicate determinations of acid-stable phosphoenzyme are shown.

rate-determining step over the complete temperature range in the reaction of this enzyme species: at decreasing temperature the following conformational transition  $\text{E}_1\text{P} \rightarrow \text{E}_2\text{P}$  is progressively contributing to rate determination of the formation of  $\text{E}_2\text{P}$ . This temperature effect could probably resolve the apparent disagreements found in the literature concerning rate determination of phosphorylation (Kane et al., 1997; Clarke et al., 1998; Keillor and Jencks, 1996).

### Activation energy for ATP phosphorylation

In a series of experiments stopped-flow RH421 fluorescence after ATP addition phosphorylation was monitored at temperatures between 5–30°C. All fluorescence responses were fitted with double-exponential time functions. As shown in Fig. 3 Arrhenius plots of the observed rate constants for the slow and fast phases in the stopped-flow fluorescence responses give significantly different slopes corresponding to activation energies  $E_a = 52.6 \pm 2.7 \text{ kJ/mol}$  for the fast phase and about half,  $25.3 \pm 6.2 \text{ kJ/mol}$ , for

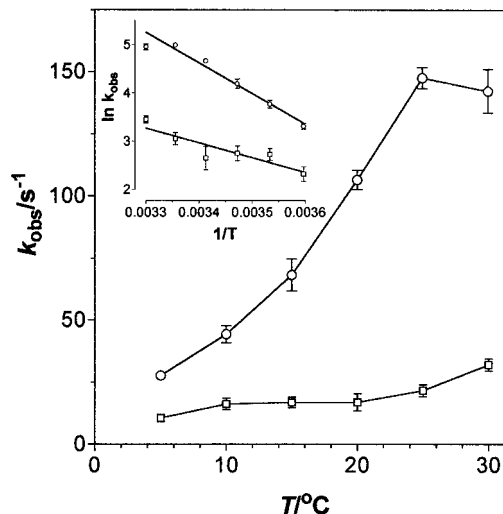


FIGURE 3 Observed rate constants ( $k_{\text{obs}}$ ) of stopped-flow RH421 fluorescence transients induced by phosphorylation from ATP (1 mM) at different temperatures. The data are means of calculated rate constants for the fast (○) and slow (□) phase for five stopped-flow experiments each collecting 4000 points fitted with double-exponential time functions. The inset shows an Arrhenius plot of the calculated rate constants for the fast (○) and slow (□) phase. The slopes of the straight lines correspond to activation energies of  $52.6 \pm 2.7 \text{ kJ/mol}$  (fast phase) and  $25.3 \pm 6.2 \text{ kJ/mol}$  (slow phase). The experiments were performed at 16 mM NaCl, 4 mM  $\text{MgCl}_2$ , 10 mM HEPES/MES, pH 7.5.

the slow phase. The different activation energies indicate that the two phases represent different reaction steps in the reaction mechanism.

### Effects of ATP and $\text{Na}^+$ concentration

The observed rate constants of both the slow and the fast phase in the double exponential fits to the stopped-flow RH421 fluorescence measurements increased with the ATP concentration at fixed  $\text{Na}^+$  concentrations (Fig. 4, A and B). For both the slow phase and the fast phase the ATP-substrate curves were significantly better fitted with second-degree equations than with simple hyperbolic equations, as clearly indicated by the curved Eadie plots given as insets to Fig. 4, A and B. The curves in Fig. 4 represent second-degree equations equivalent to the sum of two Michaelis-Menten-type equations (Cornelius and Skou, 1987):

$$k_{\text{obs}} = k_{\text{max},1} \frac{[\text{ATP}]}{K_{\text{ATP},1} + [\text{ATP}]} + k_{\text{max},2} \frac{[\text{ATP}]}{K_{\text{ATP},2} + [\text{ATP}]}$$

For the fast phase the two apparent dissociation constants for ATP ( $K_{\text{ATP}}$ ) calculated from the fit were  $K_{\text{ATP},1} = 5.4 \pm 0.3 \mu\text{M}$  and  $K_{\text{ATP},2} = 32 \pm 11 \text{ nM}$ . The higher calculated apparent dissociation constant is in the same range as previously found for ATP phosphorylations using stopped-flow RH421 fluorescent transients analyzed by simple hyperbolic binding curves that yielded dissociation constants of  $\sim 7 \mu\text{M}$  for pig kidney Na,K-ATPase (Kane et al., 1997) and  $8 \mu\text{M}$  for rabbit kidney Na,K-ATPase at 130 mM  $\text{Na}^+$

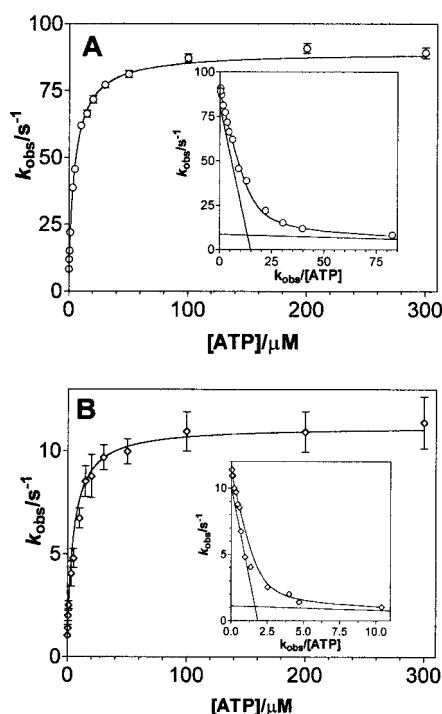


FIGURE 4 Dependence of observed rate constants ( $k_{\text{obs}}$ ) for the fast and slow phases in stopped-flow RH421 fluorescence on the concentration of ATP at 16 mM  $\text{Na}^+$ ;  $T = 20^\circ\text{C}$ . Each point represents the mean of 12 experiments, each representing the average of five stopped-flow measurements containing 4000 data points each. (A) Fit to the observed rate constants for the fast phase ( $\circ$ ) as shown by the solid curve using an equation equivalent to the sum of two Michaelis-Menten equations (Cornelius and Skou, 1987; see Results and Discussion). The fitted apparent dissociation constants for ATP were  $5.4 \pm 0.3 \mu\text{M}$  and  $23 \pm 11 \text{ nM}$ , respectively.  $k_{\text{max},1}$  and  $k_{\text{max},2}$  were  $81 \pm 1 \text{ s}^{-1}$  and  $8.7 \pm 0.7 \text{ s}^{-1}$ , respectively. The inset to (A) shows an Eadie plot of the data with the fitted equation indicated. Also shown are the two lines with negative slopes equivalent to the two apparent ATP dissociation constants. (B) The observed rate constant of the minor slow phase in the fluorescence response ( $\diamond$ ). The substrate curve could be fitted with the same relation and fitting parameters as found for the fast phase indicated by the curve.

(Clarke et al., 1998). The lower  $K_{\text{ATP}}$  value is comparable to values previously found from steady-state measurements of  $\text{Na}^+$ -ATPase activity of shark enzyme under comparable experimental conditions that gave linear Eadie plots at  $[\text{ATP}]$  up to  $50 \mu\text{M}$  with apparent dissociation constants of 80–230 nM depending on  $[\text{Na}^+]$  (Cornelius and Skou, 1987). This is a little lower than the predicted true ATP affinity for the catalytic site calculated from the proper ratio of measured rate constants (cf. Campos and Beaugé, 1994). The appearance of two ATP binding affinities could indicate that the  $\text{E}_2\text{-E}_1$  transitions without and with ATP bound proceed with different rate constants also in the absence of  $\text{K}^+$  (Post et al., 1975, Campos and Beaugé, 1994).

Values of  $k_{\text{obs}}$  for the minor slow phase in the fluorescence responses (Fig. 4 B) could be satisfactory scaled to fit the same function of  $[\text{ATP}]$  as the fast phase (Fig. 4 A) making it unlikely that the slow fluorescence phase is caused by nonspecific dye effects, as suggested by Heyse et

al. (1994). More important, the fact that  $k_{\text{obs}}$  increases with  $[\text{ATP}]$  also seems to exclude that the slow phase is caused by a slow, rate-determining  $\text{E}_2 \rightleftharpoons \text{E}_1$  transition preceding the phosphorylation reaction: if a significant  $\text{E}_2$  fraction was responsible for the slow phase in the stopped-flow RH421 fluorescence, then the observed rate constant would decrease with increasing  $[\text{ATP}]$ , since at low  $[\text{ATP}]$   $k_{\text{obs}} \rightarrow k_f + k_b$ , whereas at high  $[\text{ATP}]$   $k_{\text{obs}}$  would approach  $k_f$ . This apparently excludes that pre-formed  $\text{E}_2$  is the major course of the slow phase at  $[\text{Na}^+] \geq 16 \text{ mM}$  and limits the explanations for the slow phase to processes following the phosphorylation reactions.

Another indication that the slow phase is related to an intrinsic kinetic property of the enzyme comes from  $\text{Na}^+$  titration experiments at a constant ATP concentration. In Fig. 5 A the observed rate constants for the fast and slow phases of stopped-flow RH421 fluorescence responses to 300  $\mu\text{M}$  ATP are shown at increasing  $[\text{Na}^+]$ . The ionic strength is held constant with choline chloride. The observed rate constant for the fast phase in the double-exponential fluorescence response is clearly a sigmoidal function on the  $[\text{Na}^+]$ . The Hill coefficient for the fit is 2.2 and

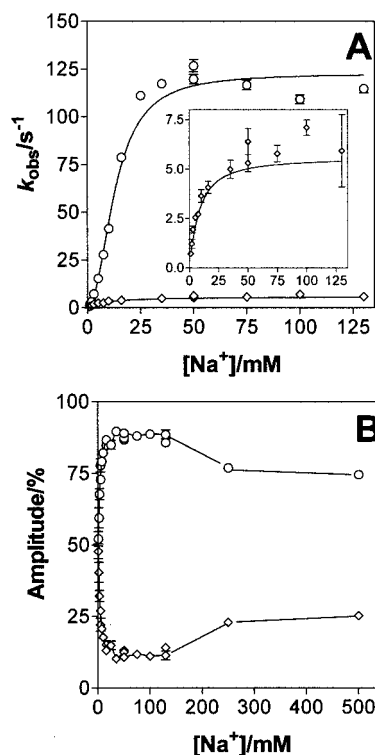


FIGURE 5 (A) Dependence of observed rate constants ( $k_{\text{obs}}$ ) for the fast ( $\circ$ ) and slow ( $\diamond$ ) phases in stopped-flow RH421 fluorescence after ATP addition on the concentration of  $\text{Na}^+$ . The inset is an enlarged figure of the slow phase. The curves are Hill equation fits to the data. The following parameters were used in the fits: for the fast phase  $n_H = 2.15 \pm 0.05$  and  $K_{0.5} = 13.1 \pm 1.0 \text{ mM}$ ; for the slow phase  $n_H = 1.2 \pm 0.2$  and  $K_{0.5} = 8.7 \pm 1.2 \text{ mM}$ . (B) Relative amplitudes of the two phases in the double-exponential fits to the stopped-flow RH421 fluorescence responses up to 500 mM  $\text{Na}^+$ . In both panels the ion strength was kept constant with choline chloride.  $T = 20^\circ\text{C}$ .

$K_{0.5} = 13$  mM. The slow phase of the stopped-flow fluorescence response is also a saturating function of the  $\text{Na}^+$  concentration as seen from the inset to Fig. 5 A. Due to the larger variation in the evaluation of the rate constant for the small slow phase it is not possible to discriminate between a sigmoidal and a hyperbolic fit to the data. The shown sigmoidal fit has a Hill coefficient of 1.2 and a  $K_{0.5} = 8.7$  mM. The results are compatible with the cooperative binding of 3  $\text{Na}^+$  ions to the  $\text{E}_1$  form, before phosphorylation by ATP. The results for the fast phase are in accord with previous results obtained by stopped-flow RH421 fluorescence using pig or rabbit kidney  $\text{Na}^+, \text{K}^+$ -ATPase (Kane et al., 1997; Clarke et al., 1998), and with results analyzing Na-ATPase activity from reconstituted shark enzyme (Cornelius and Skou, 1988). The results for the slow phase support the notion that this phase represents reactions following the phosphorylation step.

In Fig. 5 B the relative contributions of the fast and slow phases to the total fluorescence response are depicted as a function of the  $\text{Na}^+$  ion concentration. As indicated, the proportion of the slow phase decreases at increasing  $[\text{Na}^+]$  and then attains a constant value of  $\sim 20\%$  at  $[\text{Na}^+] > 10$  mM. The increase in the proportion of the slow phase at very low  $\text{Na}^+$  ion concentrations could indicate that the reaction  $\text{E}_2 \rightleftharpoons \text{E}_1$  becomes progressively important due to a shift toward  $\text{E}_2$  at low  $[\text{Na}^+]$ . This is in accord with previous results where an  $\text{E}_2/\text{E}_1$  ratio of  $\sim 1/5$  in the absence of  $\text{Na}^+$  is found (Cornelius et al., 1998). An increase in the  $\text{E}_2$  proportion at decreasing  $[\text{Na}^+]$  will appear as a relative increase of the slow phase in the double-exponential fits due to the increasing weight of the slow  $\text{E}_2 \rightarrow \text{E}_1$  transition.

### The effects of ADP

As seen from Fig. 6 increasing  $[\text{ADP}]$  progressively decreased the observed rate constant in the stopped-flow

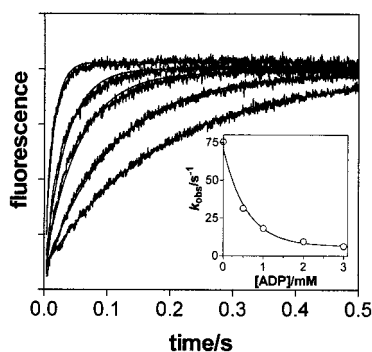


FIGURE 6 Stopped-flow RH421 fluorescence transients induced by rapid mixing of enzyme with 1 mM ATP and increasing concentrations of ADP. The upper trace is without ADP followed by 0.5, 1.0, 2.0, and 3.0 mM ADP. The steady-state fluorescence levels were measured using a Spex spectrofluorometer. All experiments were performed with 16 mM NaCl, 4 mM  $\text{MgCl}_2$ , 10 mM HEPES/MES, pH 7.5.  $T = 20^\circ\text{C}$ . The solid curves represent double-exponential fits to the data, and the inset shows the calculated rate constant for the major fast phase in the double-exponential fits as a function of  $[\text{ADP}]$ .

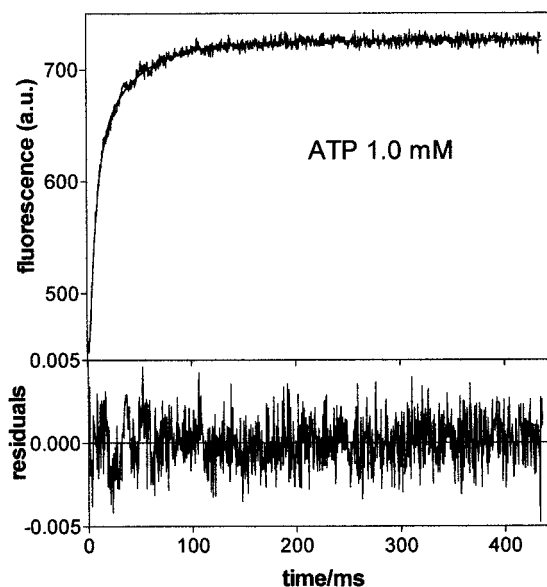


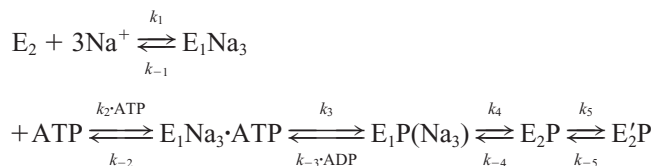
FIGURE 7 Model progress curve computed using the program DYNAFIT (16) to simulate the stopped-flow RH421 fluorescence response of shark  $\text{Na}^+, \text{K}^+$ -ATPase to the addition of 1 mM ATP in the presence of 16 mM  $\text{Na}^+$ . In the program simulation the model given in Scheme 2 is used with the following constants fixed:  $k_{-1} = 0.18 \text{ s}^{-1}$  and  $K_{\text{ATP}} = 4.5 \times 10^6 \text{ M}^{-1}$ . The fitted constants were:  $k_1 = 57 \pm 8 \text{ s}^{-1}$ ,  $k_3 = 527 \pm 42 \text{ s}^{-1}$ ,  $k_4 = 98.4 \pm 0.6 \text{ s}^{-1}$ ,  $k_{-4} = 30.0 \pm 0.4 \text{ s}^{-1}$ ,  $k_5 = 30.0 \pm 0.5 \text{ s}^{-1}$ , and  $k_{-5} \approx 0$ .

RH421 fluorescence after ATP addition. As pointed out by Keillor and Jencks (1996) this is not to be expected from a simplified reaction scheme such as  $\text{E} + \text{ATP} \rightleftharpoons \text{E} \cdot \text{ATP} \rightleftharpoons \text{EP}$ , because the observed rate constant for the phosphorylation reaction would be the sum of the first-order rate constant  $k_2$  and the pseudo-first-order rate constant  $k_{-2}[\text{ADP}]$ , assuming the second step to be rate-limiting. As  $[\text{ADP}]$  increases  $k_{\text{obs}}$  should also increase, which was clearly not the case (Fig. 6). Rather, it indicated that ADP increases the back reaction rate of a step before production of the high-fluorescent  $\text{E}_2\text{-P}$  form. It is tempting to identify this precursor as the ADP-sensitive  $\text{E}_1\text{-P}$  phosphoform. Another possibility would be a competitive inhibition of ADP on ATP binding to  $\text{E}_1$ . However, in order to simulate the significant decrease in  $k_{\text{obs}}$  vs.  $[\text{ADP}]$  shown in the inset to Fig. 6 by competitive binding of ATP and ADP an association constant for ADP binding to  $\text{E}_1$  ( $K_{\text{ADP}}$ ) as high as  $1.3 \cdot 10^8 \text{ M}^{-1}$  would have to be assumed. To investigate whether the presence of  $\text{E}_1\text{-P}$  alone, without proposing a new intermediate like  $\text{E}^* \cdot \text{ATP}$  (Keillor and Jencks, 1996) in the Albers-Post scheme is adequate to explain the kinetic data, model simulations were performed as described below.

### Model simulations

In the following the question of the origin of the slow phase in the RH421 fluorescence response to ATP was addressed. In the reaction sequence normally assumed for the ATP phosphorylation a slow  $\text{E}_2 \rightleftharpoons \text{E}_1$  step could not account for the slow phase observed in the stopped-flow experiments,

since  $k_{\text{obs}}$  for this phase increases with [ATP] (Fig. 4 B). Therefore, at the  $\text{Na}^+$  concentrations used (16 mM and 130 mM) pre-formed  $\text{E}_2$  need not be considered. In the following it was investigated whether a slow formation of a  $\text{K}^+$ -insensitive phosphoenzyme,  $\text{E}_2'\text{P}$ , formed from  $\text{E}_2\text{P}$  in the absence of  $\text{K}^+$  and with a similar high fluorescence (Klodos et al., 1997) could account for the biphasic stopped-flow RH421 fluorescence responses. This  $\text{K}^+$ -insensitive  $\text{E}_2'\text{P}$  phosphoenzyme is distinct from the  $\text{K}^+$ -sensitive  $\text{E}_2\text{P}$  phosphoform and was previously demonstrated in  $\text{P}_i$  phosphorylation studies (Cornelius et al., 1998; Post et al., 1975; Fedosova et al., 1998; Klodos et al., 1997). The idea is that phosphorylation of  $\text{E}_1$  and production of  $\text{E}_2\text{P}$  give rise to the fast phase, whereas the slow phase is produced by the slower  $\text{E}_2\text{P} \rightarrow \text{E}_2'\text{P}$  transition. The activation energies (Fig. 3) characteristic for the fast and slow phases, respectively, could then reflect the temperature sensitivity of these two reactions. To test this hypothesis, the fluorescence data were fitted with a reaction sequence incorporating the three phosphoforms and the two major conformations  $\text{E}_1$  and  $\text{E}_2$ :



Scheme 2

In the model, binding and occlusion of 3  $\text{Na}^+$  are assumed.

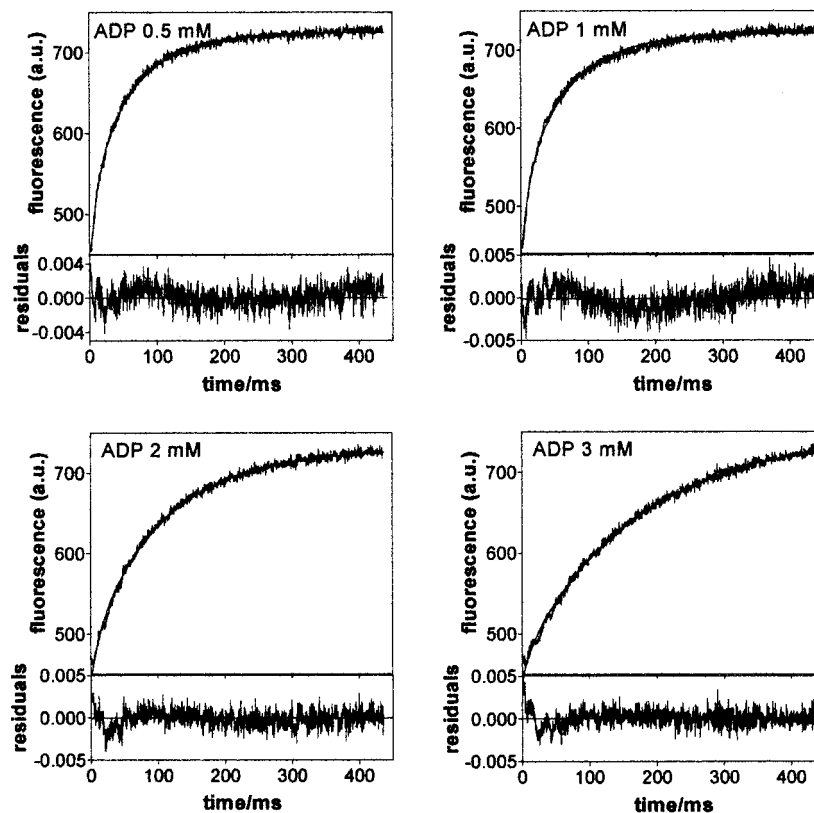
The program DYNAFIT (Kuzmic, 1996) was used to fit rate constants using the kinetic model in Scheme 2 to the stopped-flow RH421 fluorescence data after ATP phosphorylation in the absence of ADP. The following parameters were fixed:  $k_{-5} = 0.18 \text{ s}^{-1}$  (Cornelius et al., 1998),  $K_{\text{ATP}} = k_{-2}/k_2 = 4.5 \times 10^6 \text{ M}^{-1}$  (Cornelius and Skou, 1987), and  $[\text{ADP}] = 0$ . The low-affinity ATP reaction  $\text{E}_2 \rightleftharpoons \text{E}_2\text{ATP} \rightleftharpoons \text{E}_1\text{ATP}$  (Post et al., 1975; Campos and Beaugé, 1994) was not included in the simulation because an initial presence of a major  $\text{E}_2$  fraction could be ignored, as described above.

As shown in Fig. 7 an excellent fit of the model in Scheme 2 to the data could be obtained with the following rate constants:  $k_1 = 57 \pm 8 \text{ s}^{-1}$ ,  $k_3 = 527 \pm 42 \text{ s}^{-1}$ ,  $k_4 = 98 \pm 0.6 \text{ s}^{-1}$  and  $k_{-4} = 30 \pm 0.4 \text{ s}^{-1}$ , and  $k_5 = 30 \pm 0.5 \text{ s}^{-1}$ ,  $k_{-5} \approx 0$  (actually, equally good fit to the RH421 fluorescence data could be obtained with  $k_{-5}$  values up to  $\sim 12 \text{ s}^{-1}$ ).

The fitted values for  $k_1$  and  $k_3$  are within the range previously found: Skou and Esmann (1983) estimated  $k_1$  to be  $\sim 14 \text{ s}^{-1}$  at  $6^\circ\text{C}$  ( $\approx 70 \text{ s}^{-1}$  at  $20^\circ\text{C}$ ) and saturating  $[\text{Na}^+]$  using eosin, and Clarke et al. (1998) estimated  $k_1$  to be below  $39 \text{ s}^{-1}$  at  $24^\circ\text{C}$  for rabbit kidney  $\text{Na}^+, \text{K}^+$ -ATPase. The calculated phosphorylation constant ( $k_3$ ) is also in accordance with previous findings. Keillor and Jencks (1996) found a phosphorylation constant of  $\sim 460 \text{ s}^{-1}$  and Sokolov et al. (1998) found it to be  $\sim 600 \text{ s}^{-1}$ , both values measured at  $20^\circ\text{C}$ .

It should be emphasized that this explanation of the slow phase does not assume  $\text{E}_2'\text{P}$  to be an intermediate in the

FIGURE 8 Simulations of stopped-flow RH421 fluorescence responses after the addition of 1 mM ATP in the presence of 16 mM  $\text{Na}^+$  together with either 0.5, 1, 2, or 3 mM ADP to shark  $\text{Na}^+, \text{K}^+$ -ATPase. The only variable constant was  $k_{-3}$ ; all other constants were fixed to the values calculated from the fit to the data without ADP as given in Fig. 7. The fitted rate constants were  $1.62 (\pm 0.01) \times 10^6 \text{ M}^{-1} \text{ s}^{-1}$ ,  $0.95 (\pm 0.01) \times 10^6 \text{ M}^{-1} \text{ s}^{-1}$ ,  $1.09 (\pm 0.01) \times 10^6 \text{ M}^{-1} \text{ s}^{-1}$ , and  $1.4 (\pm 0.01) \times 10^6 \text{ M}^{-1} \text{ s}^{-1}$ , respectively, when ADP increased from 0.5 mM to 3 mM.



physiological reaction cycle of the  $\text{Na}^+, \text{K}^+$ -ATPase. First, in the presence of  $\text{K}^+$  the main reaction route would be via dephosphorylation of  $\text{E}_2\text{P} \rightleftharpoons \text{E}_2(\text{K}_2) + \text{P}_i$ , which has a forward rate constant of  $\sim 300 \text{ s}^{-1}$  (Kane et al., 1998; Mårdh and Zetterqvist, 1974; Hobbs et al., 1980) and the much slower  $\text{E}_2\text{P} \rightleftharpoons \text{E}'_2\text{P}$  transition would be effectively bypassed. Second, in the absence of  $\text{K}^+$  where the dephosphorylation reaction is rate-limiting, no deviations from previous schemes would result because the spontaneous dephosphorylation rate for the two  $\text{E}_2\text{P}$  phosphoenzymes has been found to be identical (Cornelius et al., 1998) and  $\sim 1.1 \text{ s}^{-1}$  at  $20^\circ\text{C}$ . Finally, very slow phases, which could be indicative of the  $\text{K}^+$ -insensitive  $\text{E}'_2\text{P}$ , have previously been identified in  $\text{K}^+$ -supported dephosphorylation at both  $21^\circ\text{C}$  (Froehlich and Fendler, 1991) and  $0^\circ\text{C}$  (Cornelius, 1995) after ATP phosphorylation in the absence of  $\text{K}^+$ . Clarke et al. (1998) offer another model, which is also compatible with biphasic fluorescence responses. In this, the fast fluorescence phase is associated with the rapid  $\text{Na}^+$  dissociation from  $\text{E}_2\text{P}$  (rate-limited by a combination of the phosphorylation step and the  $\text{E}_1\text{P} \rightarrow \text{E}_2\text{P}$  conformational step) and the slow phase is due to the relaxation of the dephosphorylation/phosphorylation equilibrium (limited by the  $\text{E}_2 \rightarrow \text{E}_1$  transition). This model, furthermore, assumes that fluorescence of RH421 associated with  $\text{E}_2$  and  $\text{E}_2\text{P}$  states is equally high. However, attempts to use this model gave poor fits to the present data for shark enzyme with unrealistic fitted rate constants unless  $>10\%$  pre-formed  $\text{E}_2$  was assumed, which is considered unlikely, at least at  $[\text{Na}^+] \geq 16 \text{ mM}$ .

A third alternative explanation for the biphasic fluorescence responses could be the assignment of different fluorescence levels to  $\text{E}_2\text{P}$  species depending on their relative saturation with  $\text{Na}^+$  and assuming one of the  $\text{Na}^+$  release steps to be slow. However, such a model assuming one of the  $\text{Na}^+$  release steps to be slow compared to the  $\text{E}_1\text{P} \rightarrow \text{E}_2\text{P}$  conformational transition is unlikely, since the release of  $\text{Na}^+$  from  $\text{E}_2\text{P}$  is found to be very fast ( $700\text{--}5000 \text{ s}^{-1}$  (Wuddel and Apell, 1995; Wagg et al., 1997)).

The next step was to confirm that using the fitted rate constants of the reaction model described by Scheme 2 in the absence of ADP, the stopped-flow RH421 fluorescence results obtained at varying  $[\text{ADP}]$  could be satisfactorily fitted with  $k_{-3}$  as the only variable fit parameter. The results are shown in Fig. 8, and as seen this is actually possible. In these fits  $k_{-3}$  varied insignificantly between  $0.95 \times 10^6$  and  $1.6 \times 10^6 \text{ M}^{-1} \text{ s}^{-1}$ , giving an intrinsic site constant for ADP of  $\sim 2.5 \times 10^3 \text{ M}^{-1}$ . This value is identical to the one found by Sokolov et al. (1998) from transient current measurements induced by photochemically released caged ATP in rabbit kidney enzyme capacitatively coupled to planar bilayers.

Finally, in Fig. 9 the fitted rate constants in Scheme 2 were used to simulate both the stopped-flow RH421 fluorescence responses assuming  $\Delta F/F_0$  to be proportional to  $(\text{E}_2\text{P} + \text{E}'_2\text{P})$  (Fig. 9 A) and the quenched-flow responses assuming  $\text{EP} = (\text{E}_1\text{P} + \text{E}_2\text{P} + \text{E}'_2\text{P})$  (Fig. 9 B). As seen, it was possible with this model to accurately simulate the observed ADP inhibition patterns given in Fig. 6 with a

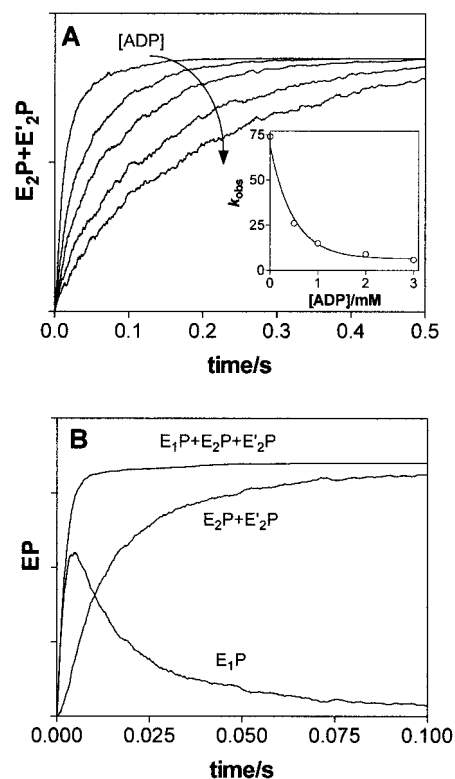


FIGURE 9 Model simulations of phosphoenzyme levels using the reaction given in Scheme 2 with  $[\text{ATP}] = 1 \text{ mM}$  and the rate constants given in Fig. 7, and a  $k_{-3}$  value as found in Fig. 8. In (A) simulated levels of  $(\text{E}_2\text{P} + \text{E}'_2\text{P})$ , which are both assumed to be highly fluorescent, are shown at increasing ADP concentrations of 0, 0.5, 1, 2, and 3 mM. The inset shows the calculated rate constants for the fast phase in double-exponential fits to the curves vs.  $[\text{ADP}]$ . In (B) calculated levels of phosphoenzyme combinations  $(\text{E}_2\text{P} + \text{E}'_2\text{P})$ ,  $\text{E}_1\text{P}$ , and  $(\text{E}_1\text{P} + \text{E}_2\text{P} + \text{E}'_2\text{P})$  are shown using Scheme 2 and the fitted rate constants.  $(\text{E}_2\text{P} + \text{E}'_2\text{P})$  reflects the stopped-flow RH421 fluorescence responses, whereas  $(\text{E}_1\text{P} + \text{E}_2\text{P} + \text{E}'_2\text{P})$  is the acid-stable phosphoenzymes measured in the quenched-flow experiments. The program Chemical Kinetic Simulator (IBM) was used to simulate the enzyme species in the model.

decrease in  $k_{\text{obs}}$  at increasing  $[\text{ADP}]$ . Also, the qualitative difference in the rate of RH421 fluorescence and production of acid-stable EP after ATP phosphorylation where the appearance of acid-stable phosphoenzyme precedes RH421 fluorescence, as shown in Fig. 2, could be simulated.

To conclude, the present results are compatible with a model in which the phosphorylation by ATP of shark rectal gland enzyme as detected by the stopped-flow RH421 fluorescence is caused by a high fluorescence of RH421 associated with the  $\text{E}_2\text{P}$  and  $\text{E}'_2\text{P}$  conformations, whereas RH421 associated with other enzyme conformations are low or nonfluorescent. The biphasic fluorescence response to ATP phosphorylation was found to be an intrinsic kinetic property of the protein-substrate interaction. It could be explained assuming phosphorylation of  $\text{E}_1$  and subsequent formation of  $\text{E}_2\text{P}$  to cause the major fast phase in the fluorescence response, whereas the minor slow phase in the fluorescence response is attributed to the slow  $\text{E}_2\text{P} \rightleftharpoons \text{E}'_2\text{P}$  transition. The two reactions have different activation ener-

gies of 53 kJ/mol and 25 kJ/mol, respectively. The two phases in the fluorescence response were identical saturating functions of [ATP] with both low and high apparent ATP affinities excluding that the slow phase could be due to a preceding  $E_2 \rightarrow E_1$  transition. Over the temperature range 5–15°C the quenched-flow responses to ATP phosphorylation are appreciably faster than the stopped-flow RH421 fluorescence responses, demonstrating that over this temperature range the phosphorylation and the subsequent  $E_1P \rightarrow E_2P$  conformational transition contribute to rate determination of the formation of  $E_2P$ . The reaction of ADP with the fast initially formed  $E_1P$  explains the kinetics of RH421 fluorescence in the simultaneous presence of both ATP and ADP within the classical Albers-Post scheme.

Hanne R. Z. Christensen and Henriette R. Petersen are greatly acknowledged for excellent technical assistance and Drs K. Fendler, I. Klodos and N. U. Fedosova for valuable discussions.

## REFERENCES

- Albers, R. W. 1967. Biochemical aspects of active transport. *Annu. Rev. Biochem.* 36:727–756.
- Bühler, R., W. Stürmer, H.-J. Apell, and P. Läuger. 1991. Charge translocation by the Na,K-pump. I. Kinetics of local field changes studied by time-resolved fluorescence measurements. *J. Membr. Biol.* 121:141–161.
- Campos, M., and L. Beaugé. 1994.  $Na^+$ -ATPase activity of  $Na^+, K^+$ -ATPase. *J. Biol. Chem.* 269:18028–18036.
- Clarke, R. J., D. J. Kane, H.-J. Apell, M. Roudna, and E. Bamberg. 1998. Kinetics of  $Na^+$ -dependent conformational changes of rabbit kidney  $Na^+, K^+$ -ATPase. *Biophys. J.* 75:1340–1353.
- Cornelius, F. 1995. Cholesterol modulation of molecular activity of reconstituted shark  $Na^+, K^+$ -ATPase. *Biochim. Biophys. Acta.* 1235:197–204.
- Cornelius, F. 1996. The sodium pump. In *Biomembranes*, Vol. 5. A. G. Lee, editor. JAI Press, Greenwich, CT. 133–184.
- Cornelius, F., N. U. Fedosova, and I. Klodos. 1998.  $E_2P$  phosphoforms of Na,K-ATPase. II. Interaction of substrate and cation binding sites in Pi-phosphorylation of Na,K-ATPase. *Biochemistry.* 37:16686–16696.
- Cornelius, F., and J. C. Skou. 1987. The sided action of  $Na^+$  and of  $K^+$  on reconstituted shark ( $Na^+ + K^+$ )-ATPase engaged in  $Na^+ - Na^+$  exchange accompanied by ATP hydrolysis. I. The ATP activation curve. *Biochim. Biophys. Acta.* 904:353–364.
- Cornelius, F., and J. C. Skou. 1988. The sided action of  $Na^+$  on reconstituted shark ( $Na^+ + K^+$ )-ATPase engaged in  $Na^+ - Na^+$  exchange accompanied by ATP hydrolysis. II. Transmembrane allosteric effects on  $Na^+$  affinity. *Biochim. Biophys. Acta.* 944:223–232.
- Fedosova, N. U., F. Cornelius, and I. Klodos. 1995. Fluorescent styryl dyes as probes for Na,K-ATPase reaction mechanism. Significance of the charge of the hydrophilic moiety of RH-dyes. *Biochemistry.* 34:16806–16814.
- Fedosova, N. U., F. Cornelius, and I. Klodos. 1998.  $E_2P$  phosphoforms of Na,K-ATPase. I. Comparison of intermediates formed from ATP and Pi. The reactivity towards vanadate and hydroxylamine. *Biochemistry.* 37:13634–13642.
- Forbush, B., and I. Klodos. 1991. Rate-limiting steps in Na translocation by the Na/K pump. In *The Sodium Pump. Structure, Mechanism, and Regulation*. J. H. Kaplan and P. De Weer, editors. Rockefeller University Press, New York. 211–225.
- Frank, J., A. Zouni, A. van Hoek, A. J. W. G. Visser, and R. J. Clarke. 1996. Interaction of the fluorescent probe RH421 with ribulose-1,5-bisphosphate carboxylase/oxygenase and with  $Na^+, K^+$ -ATPase membrane fragments. *Biochim. Biophys. Acta.* 1280:51–64.
- Froehlich, J. P., and K. Fendler. 1991. The partial reactions of the  $Na^+$  and  $Na^+ + K^+$ -activated adenosine triphosphatases. In *The Sodium Pump. Structure, Mechanism, and Regulation*. J. H. Kaplan and P. De Weer, editors. Rockefeller University Press, New York. 227–247.
- Heyse, S., I. Wuddel, H.-J. Apell, and W. Stürmer. 1994. Partial reactions of the Na,K-ATPase: determination of rate constants. *J. Gen. Physiol.* 104:197–240.
- Hobbs, A. S., R. W. Albers, and J. P. Froehlich. 1980. Potassium-induced changes in phosphorylation and dephosphorylation of ( $Na^+ + K^+$ )-ATPase observed in the transient state. *J. Biol. Chem.* 255:3395–3402.
- Jencks, W. P. 1983. What is a coupled vectorial process? *Curr. Top. Memb. Transp.* 19:1–19.
- Kane, D. J., K. Fendler, E. Grell, E. Bamberg, K. Taniguchi, J. P. Froehlich, and R. J. Clarke. 1997. Stopped-flow kinetic investigations of conformational changes of pig kidney  $Na^+, K^+$ -ATPase. *Biochemistry.* 36:13406–13420.
- Kane, D. J., E. Grell, E. Bamberg, and R. J. Clarke. 1998. Dephosphorylation kinetics of pig kidney  $Na^+, K^+$ -ATPase. *Biochemistry.* 37:4581–4591.
- Keillor, J. W., and W. P. Jencks. 1996. Phosphorylation of the sodium-potassium adenosinetriphosphatase proceeds through a rate-limiting conformational change followed by a rapid phosphoryl transfer. *Biochemistry.* 35:2750–2753.
- Klodos, I. 1994. Partial reactions in  $Na^+/K^+$ - and  $H^+/K^+$ -ATPase studied with voltage-sensitive fluorescent dyes. In *The Sodium Pump: Structure, Mechanism, Hormonal Control, and Its Role in Disease*. E. Bamberg and W. Schoner, editors. Steinkopff, Darmstadt. 517–528.
- Klodos, I., N. U. Fedosova, and F. Cornelius. 1997. Fluorescent styryl dyes as probes for Na,K-ATPase reaction: enzyme source and fluorescence response. In *Na/K-ATPase and Related Transport ATPases: Structure, Mechanism, and Regulation*. L. A. Beaugé, D. C. Gadsby, and P. J. Garrahan, editors. *Ann. NY Acad. Sci.* 834:394–396.
- Kuzmic, P. 1996. Program dynafit for the analysis of enzyme kinetic data: application to HIV proteinase. *Anal. Biochem.* 237:260–273.
- Lowry, O. H., N. J. Rosebrough, A. L. Farr, and R. J. Randall. 1951. Protein measurement with the Folin phenol reagent. *J. Biol. Chem.* 193:265–275.
- Mårdh, S., and Ö. Zetterqvist. 1974. Phosphorylation and dephosphorylation reactions of bovine brain ( $Na^+ + K^+$ )-stimulated ATP phosphohydrolase studied by rapid-mixing technique. *Biochim. Biophys. Acta.* 350:473–483.
- Ottolenghi, P. 1975. The reversible delipidation of a solubilized sodium-plus-potassium ion-dependent adenosine triphosphatase from the salt gland of the spiny dogfish. *Biochem. J.* 151:61–66.
- Post, R. L., T. Kume, T. Tobin, B. Orcutt, and A. K. Sen. 1969. Flexibility of an active centre in sodium-plus-potassium adenosine triphosphatase. *J. Gen. Physiol.* 54:306–326.
- Post, R. L., G. Toda, and F. N. Rogers. 1975. Phosphorylation by inorganic phosphate of sodium plus potassium ion transport adenosine triphosphatase. *J. Biol. Chem.* 250:691–701.
- Pratap, P. R., and J. D. Robinson. 1993. Rapid kinetic analyses of the  $Na^+/K^+$ -ATPase distinguish among different criteria for conformational change. *Biochim. Biophys. Acta.* 1151:89–98.
- Skou, J. C. 1992. The Na-K pump. *NIPS.* 7:95–100.
- Skou, J. C., and M. Esmann. 1983. The effects of  $Na^+$  and  $K^+$  on the conformational transitions of ( $Na^+ + K^+$ )-ATPase. *Biochim. Biophys. Acta.* 746:101–113.
- Skou, J. C., and M. Esmann. 1988. Preparation of membrane  $Na^+, K^+$ -ATPase from rectal glands of *Squalus acanthias*. *Methods Enzymol.* 156:43–46.
- Sokolov, V. S., H.-J. Apell, J. E. T. Corrie, and D. R. Trentham. 1998. Fast transient currents in Na,K-ATPase induced by ATP concentration jumps from the  $P^3$ -[3',5'-dimethoxyphenyl]-2-phenyl-2-oxoethyl ester of ATP. *Biophys. J.* 74:2285–2298.
- Stürmer, W., R. Bühler, H.-J. Apell, and P. Läuger. 1991. Charge translocation by the Na,K-pump. II. Ion binding and release at the extracellular face. *J. Membr. Biol.* 121:163–176.
- Wagg, J., M. Holmgren, D. C. Gadsby, J. Bezanilla, R. J. Rakowski, and P. De Weer. 1997. Na/K pump-mediated charge movements reporting deocclusion of 3  $Na^+$ . *Biophys. J.* 72:25a. (Abstr.).
- Wuddel, I., and H.-J. Apell. 1995. Electrogenicity of the sodium transport pathway in the Na,K-ATPase probed by charge-pulse experiments. *Biophys. J.* 69:909–921.